

GAMMA-RAY BURST SPECTRUM WITH DECAYING MAGNETIC FIELD

XIAOHONG ZHAO^{1,2,4}, ZHUO LI^{3,2}, XUEWEN LIU^{4,5}, BINBIN ZHANG⁴, JINMING BAI^{1,2} AND PETER MÉSZÁROS⁴
Draft version November 2, 2018

ABSTRACT

In the internal shock model for gamma-ray bursts (GRBs), the synchrotron spectrum from the fast cooling electrons in a homogeneous downstream magnetic field (MF) is too soft to produce the low-energy slope of GRB spectra. However the magnetic field may decay downstream with distance from the shock front. Here we show that the synchrotron spectrum becomes harder if electrons undergo synchrotron and inverse-Compton cooling in a decaying MF. To reconcile this with the typical GRB spectrum with low energy slope $\nu F_\nu \propto \nu$, it is required that the postshock MF decay time is comparable to the cooling time of the bulk electrons (corresponding to a MF decaying length typically of $\sim 10^5$ skin depths); that the inverse-Compton cooling should dominate synchrotron cooling after the MF decay time; and/or that the MF decays with comoving time roughly as $B \propto t^{-1.5}$. An internal shock synchrotron model with a decaying MF can account for the majority of GRBs with low energy slopes not harder than $\nu^4/3$.

Subject headings: gamma ray: bursts — gamma ray: observations

1. INTRODUCTION

The radiation mechanism of gamma-ray bursts (GRBs) is still one of the key problems in GRB physics. The GRB spectra usually can be well fit by the Band function (Band et al. 1993), where two power law sections are smoothly jointed. The low and high energy photon indices are typically $\alpha \sim -1$ and $\beta \sim -2.2$, respectively, and the νF_ν spectral peak energy is $E_p \sim 250$ keV. (Preece et al. 2000). Given the non-thermal spectra and the high luminosity of GRBs, it is widely believed that the main radiation mechanisms at work are synchrotron and/or inverse-Compton (IC) radiations (Mészáros et al. 1994, Tavani 1996, Cohen et al. 1997). Since the spectral bump in sub-MeV range dominates the energy flux, synchrotron is more favored over IC to account for the sub-MeV emission (Derishev et al. 2001; Piran et al. 2009).

However, more careful studies have raised questions about the simple synchrotron model. In the widely used internal shock model (Rees & Mészáros 1994), the energy dissipation in GRBs is caused by collisions between different parts of the unsteady outflow. These collisions produce shocks which accelerate electrons and generate magnetic field, and the GRB prompt emission is produced by the synchrotron radiation from the accelerated electrons. The high energy spectral slope $\beta \sim -2.2$ is consistent with the synchrotron spectrum from fast cooling electrons injected as a power law energy distribution with the particle index $p \sim 2.3$, a typical value in

Fermi shock acceleration. However, in order to produce synchrotron photon of E_p at \sim sub-MeV range, the magnetic field strength should be strong, close to equipartition value. The strong fast cooling of electrons in strong magnetic field produces a low energy spectral slope with $\alpha = -3/2$, extending from the injection energy E_p down to very low energy, much softer than observed ones. This raises the fast cooling problem of synchrotron radiation in GRBs (Ghisellini et al. 2000, Preece et al. 2000).

In recent years an alternative model based on photospheric emission has been widely discussed for explaining the prompt emission (Mészáros & Rees, 2000; Rees & Mészáros 2005; Ryde 2005; Pe’er et al. 2006; Beloborodov 2010). In general a hard spectrum, as hard as $\nu F_\nu \propto \nu^3$, may be produced. A number of GRBs are found to be consistent with photospheric emission (e.g., Ryde et al. 2010; Pe’er, et al. 2012). However, the spectrum predicted can be too hard at low energies and too soft at high energies, compared with typical spectral slopes of $\alpha \sim -1$ and $\beta \sim -2.2$. So a non-thermal emission component may still play a crucial role in the prompt emission.

An underlying assumption in the traditional synchrotron internal shock model is that the downstream magnetic field (MF) is homogeneous. However, as discussed by Gruzinov & Waxman (1999) and Gruzinov (2001) in the case of afterglow shocks, if the MF is generated by the Weibel instability, the MF would maintain an equipartition value only within a skin depth of the plasma, c/ω_p , where ω_p is the proton plasma frequency. The detailed processes of particle acceleration and MF formation in collisionless shock are still unclear, but numerical simulations are making progress. Recent simulations of shocks indicate that the Weibel instability induced filaments merge and cause the MF to gradually decay (e.g., Chang et al. 2008; Silva, et al. (2003); Medvedev et al. (2005)). The particle-in-cell (PIC) simulation of Chang et al. (2008) indicates that the MF decays as a power law of time. The longer PIC simulation by Keshet et al. (2009) up to $\sim 10^4 \omega_p^{-1}$ seems

¹ National Astronomical Observatories/Yunnan Observatory, Chinese Academy of Sciences, P.O. Box 110, 650011 Kunming, China; zhaohx@ynao.ac.cn

² Key Laboratory for the Structure and Evolution of Celestial Bodies, Chinese Academy of Sciences, P.O. Box 110, 650011 Kunming, China

³ Department of Astronomy and Kavli Institute for Astronomy and Astrophysics, Peking University, Beijing 100871, China; zhuo.li@pku.edu.cn

⁴ Department of Astronomy & Astrophysics and Department of Physics, The Pennsylvania State University, University Park, PA 16802, USA

⁵ Department of Physics, Sichuan University, Chengdu 610065, China

to suggest an exponential decay to $\epsilon_B \sim 10^{-2}$ at a few hundreds skin depths from the shock front. However, all the simulations currently only probe a region much smaller than the shocked region. Thus the MF evolution on longer time or space scales is still unknown.

Given the uncertainty in MF evolution behind shocks, Rossi & Rees (2003) and Lemoine (2013) have investigated the effect of MF decay on afterglow emission. Lemoine et al. (2013) use Fermi-LAT detected GRB afterglows to constrain the MF decay in large scale. Pe'er & Zhang (2006) consider the MF decay effect on the GRB prompt emission, and argue that for short enough MF decaying length scale, the electrons become slow cooling, avoiding the strong fast cooling problem in GRB spectrum. Derishev (2007) also points out that MF decay behind the shock brings flexibility for the fast cooling spectrum. Recently, Uhm & Zhang (2013) also introduce the MF decay to solve the fast cooling problem, but in a picture different from the internal shock model.

Although Pe'er & Zhang (2006) have pointed out that the extreme fast cooling slope can be avoided with MF decay, one still needs to further carefully consider how the synchrotron spectrum changes with a varying MF structure, as well as the role of IC cooling. In this paper, we carry out numerical calculation to study the effect of the decay of downstream MF on the electron cooling process and on shaping the GRB spectrum. In §2, the model of electron cooling in decaying MF is presented; §3 is the analytical analysis of the synchrotron spectrum; the results of numerical calculation of the time-integrated synchrotron and IC spectra are shown in §4; and §5 is conclusion and discussion.

2. MODEL

We consider the internal shock model for GRBs. When two parts of the GRB ejecta with different velocities collide, shock waves are generated and propagate into the unshocked ejecta. Electrons are accelerated at and near the shock front, and then produce synchrotron and IC radiation during flowing downstream. We assume the shock produced MF decay with distance away from the shock front. The exact MF structure downstream is unclear, but as some authors did (Lemoine, 2013; Medvedev & Spitkovsky 2009), we take the following two possible MF structure downstream. One is a power law decay (PLD) with time, where the magnetic field in the rest frame of the downstream plasma is

$$B = \begin{cases} B_0 & t \leq t_B \\ B_0(t/t_B)^{-\alpha_B} & t > t_B \end{cases} \quad (\text{PLD}), \quad (1)$$

and the other is an exponential decay (ED) with time,

$$B = B_0 \exp(-t/t_B) \quad (\text{ED}). \quad (2)$$

Here t is the time measured in the rest frame of the downstream plasma since the entry at the shock front. The values of the constants B_0 and t_B are presented below.

Consider a GRB with observed luminosity L and variability time δt , and assume that the bulk Lorentz factor is Γ and that the fraction of internal energy carried by accelerated electrons is ϵ_e . The internal shock radius is estimated to be $r = 2\Gamma^2 c \delta t$, and the electron number density (or proton number density) in the rest frame of the outflow is given by $n_e = L/\Gamma^2 4\pi r^2 m_p c^3 \epsilon_e$.

The MF generated by the shock is assumed to carry a fraction ϵ_B of the post-shock internal energy, thus the postshock MF at the shock front is $B_0 = \sqrt{8\pi\epsilon_B m_p c^2 n_e} = 5 \times 10^4 L_{52}^{1/2} \delta t_{-2}^{-1} (\frac{\Gamma}{300})^{-3} (\frac{\epsilon_e}{0.3})^{-1/2} (\frac{\epsilon_B}{0.3})^{1/2} \text{G}$, where the convention $Q = 10^x Q_x$ is used.

If an electron with injection Lorentz factor γ_m only cools by synchrotron radiation in the magnetic field of B_0 , the synchrotron cooling time is $\tilde{t}_c = 6\pi m_e c / \sigma_T \gamma_m B_0^2 = 3 \times 10^{-4} L_{52}^{-1} \delta t_{-2}^2 (\frac{\Gamma}{300})^6 (\frac{\epsilon_e}{0.3}) (\frac{\epsilon_B}{0.3})^{-1} \gamma_m^{-1} \text{s}$. This is much shorter than the outflow dynamical time, $t_{dyn} \simeq r/c\Gamma = 10(\Gamma/300)\delta t_{-2} \text{s}$, but much longer than the downstream plasma time scale, $\omega_p^{-1} = (4\pi n_e q_e^2 / m_p)^{-1/2} = 1.6 \times 10^{-9} L_{52}^{-1/2} \delta t_{-2} (\frac{\Gamma}{300})^3 (\frac{\epsilon_e}{0.3})^{1/2} \text{s}$. We parameterize the MF decay time t_B by

$$\tau_B \equiv t_B / \tilde{t}_c. \quad (3)$$

The Fermi shock accelerated electrons are expected to be a power law distribution, $dn_e/d\gamma_e \propto \gamma_e^{-p}$, where $\gamma > \gamma_m$ and $p \approx 2.3$. To reconcile with the observed peak energy in the sub-MeV band, the minimum electron Lorentz factor should be $\gamma_m \sim 10^3$. In the numerical calculation we will take

$$\gamma_m = 10^3 \text{ and } B_0 = 5 \times 10^4 \text{G}. \quad (4)$$

The simulation of Keshet et al. (2009) indicated $\tau_B > 10^4 \omega_p^{-1} / \tilde{t}_c \sim 0.1$. In our numerical calculation here, we will take the value of $0.1 \leq \tau_B < 5$. The MF decaying slope in the PLD case, α_B , is unclear, and here we adopt nominal values of $0.5 < \alpha_B < 3$, including the values implied by numerical simulations (Chang et al. 2008).

Since we are interested in the time-integrated emission during the electron cooling, we consider impulsive injection of high energy electrons at the shock front, and the electrons undergo synchrotron and IC cooling when being carried away downstream from the shock front. The evolution of electron energy distribution can be solved using the continuity equation,

$$\frac{\partial (dn_e/d\gamma_e)}{\partial t} + \frac{\partial [\dot{\gamma}_e (dn_e/d\gamma_e)]}{\partial \gamma_e} = 0. \quad (5)$$

The initial energy distribution of electrons follows a power law with particle index of $-p$. The time t is measured in the rest frame of the downstream plasma, starting from the injection at the shock front. When the electrons are advecting downstream they encounter a decaying MF, where the initial MF strength at injection is B_0 . Note that we neglect the adiabatic energy loss in the continuity equation, which is valid given that the radiative cooling is much faster than the expansion, as seen by $\tilde{t}_c \ll t_{dyn}$.

The radiative energy loss of the electrons can be described by

$$\dot{\gamma}_e m_e c^2 = -(P_{syn} + P_{IC}) = -\frac{4}{3} \sigma_T c \gamma_e^2 \frac{B^2}{8\pi} (1 + Y), \quad (6)$$

where $Y = P_{IC}/P_{syn}$ is the Compton parameter, and should be function of time. For simplicity, we assume that the synchrotron photon energy density that the electrons encounter during the cooling process is independent

of time t . This assumption is valid based on the following arguments. Although we consider, from technical point of view, impulsive injection of electrons in the calculation, the injection in reality happens in a finite duration, in which the shock wave crosses the colliding ejecta shell. The electrons encounter photons emitted both by earlier and later injected electrons. Moreover, the photon energy density at a certain position is contributed by photons emitted from the whole emission region. Thus, the synchrotron photon energy density is more or less constant, i.e., independent of the distance from the shock front. We will also neglect the Klein-Nishina (KN) effect in the IC scattering, and only use Thompson scattering cross section in deriving the electron cooling rate $\dot{\gamma}$. The KN effect gives a marginal correction for injection electrons around γ_m , and it is even less important when electrons cool down to lower Lorentz factors. The KN effect may have stronger effect on electrons injected with much higher energy, affecting the high energy photon index β , which is not the focus in this work. Therefore, we take

$$Y = \frac{u_{syn}}{u_B} = Y_0 \left(\frac{B_0}{B} \right)^2, \quad (7)$$

where $Y_0 = u_{syn}/(B_0^2/8\pi)$, denoting the initial ratio of IC to synchrotron power at shock front. We use the values of $Y_0 = 0.5 - 5$ in the numerical calculation.

From the above model we can solve the electron energy distribution evolving with time, and hence calculate the time-integrated synchrotron spectrum. In order to calculate the IC spectrum, one needs the energy distribution of the seed photons. Here the energy density of the seed photons, for which we only consider the synchrotron photons, is given by Y_0 and B_0 , i.e., $u_{syn} = Y_0 B_0^2/8\pi$. The spectral shape of the seed photons, based on the arguments and assumption above, is approximated by the time-integrated synchrotron photon spectrum.

3. ANALYTICAL CONSIDERATIONS

Before carrying out the numerical calculation, let us analyze analytically the low energy spectral index in the extreme cases.

Consider first the usual homogeneous MF case. We can approximate the simultaneous synchrotron spectrum from a single electron as a δ function at the characteristic synchrotron frequency $\nu(\gamma_e) \propto \gamma_e^2$ at any given time during the electron cooling. Since the cooling time is $t_c \propto \gamma_e^{-1}$, the time-integrated energy spectrum should be $\nu F_\nu t_c \propto \gamma_e \propto \nu^{1/2}$, which spans between the cooling frequency and the injection frequency.

Next consider the MF decay cases. Since the ED case is not trivial to analyze analytically, we consider here the PLD case. The electron is subject to both synchrotron and IC cooling. For simplicity we further separate the PLD case into two approximate regimes, the synchrotron-only and the IC-only cases.

For the synchrotron-only case, we have $\frac{d\gamma_e(t)}{dt} \propto \gamma_e(t)^2 B(t)^2 \propto \gamma_e(t)^2 t^{-2\alpha_B}$, and hence

$$\gamma_e \propto \begin{cases} t^{2\alpha_B-1} & \alpha_B < 1/2 \\ \text{const.} & \alpha_B > 1/2 \end{cases}. \quad (8)$$

For $\alpha_B > 1/2$, the MF decays too fast for the electron to cool, which is less interesting for GRB prompt emission

since huge energy budget would be required. The characteristic synchrotron peak frequency $\nu \propto \gamma_e^2 B(t)$ and the time (Δt) within which the electrons mainly emit synchrotron photons at ν are

$$\nu \propto \begin{cases} t^{3\alpha_B-2} & \alpha_B < 1/2 \\ t^{-\alpha_B} & \alpha_B > 1/2 \end{cases}, \quad (9)$$

$$\Delta t \propto \begin{cases} \nu^{\frac{1}{3\alpha_B-2}} & \alpha_B < 1/2 \\ \nu^{-\frac{1}{\alpha_B}} & \alpha_B > 1/2 \end{cases}. \quad (10)$$

The time-integrated energy flux is then

$$\nu F_\nu \Delta t \propto \begin{cases} \nu^{\frac{2\alpha_B-1}{3\alpha_B-2}} & \alpha_B < 1/2 \\ \nu^{2-\frac{1}{\alpha_B}} & \alpha_B > 1/2 \end{cases}, \quad (11)$$

where $F_\nu \propto B$ is used. Note the spectrum is harder than a slope of 4/3 if $\alpha_B > 3/2$, which is impossible for synchrotron spectrum. This is due to the δ function approximation of the synchrotron spectrum. Thus, in this case we should use $\nu F_\nu \Delta t \propto \nu^{4/3}$.

For the IC-only case,

$$\gamma_e \propto t^{-1}, \quad \nu \propto \gamma_e^2 B \propto t^{-(2+\alpha_B)}, \quad \Delta t \propto \nu^{-\frac{1}{2+\alpha_B}}. \quad (12)$$

The time-integrated synchrotron spectrum is

$$\nu F_\nu \Delta t \propto \nu^{\frac{2\alpha_B+1}{\alpha_B+2}}. \quad (13)$$

Note the spectrum is harder than a slope of 4/3 if $\alpha_B > 5/2$, in which we should also use $\nu F_\nu \Delta t \propto \nu^{4/3}$.

From equations (11) and (13) (also see Lemoine 2013 and Derishev 2007 for similar derivations), one finds that if $\alpha_B = 0$, we recover the usual spectrum fast cooling spectral slope of 1/2. However, if the MF decays, $0 < \alpha_B < 2/3$, the spectrum in the synchrotron only case becomes softer than 1/2 (eq [11]); while, on the contrary, in the IC-only case the spectrum becomes harder than 1/2, and the larger α_B the harder the spectrum (eq [13]). Thus, IC cooling is important in producing a hard spectrum.

4. NUMERICAL RESULTS

We present here our numerical results for the GRB spectra. We take the case with the parameter values of $\alpha_B = 1.5$, $\tau_B = 1.0$, $Y_0 = 0.5$ and $p = 2.3$ as the fiducial model, which gives a time-integrated synchrotron spectrum consistent with the typical GRB spectrum with $\alpha \sim -1$ ($\nu F_\nu \propto \nu$). The calculation is carried out in the rest frame of the plasma downstream, but the resultant spectra have been plotted in the observer frame using a typical bulk Lorentz factor $\Gamma = 300$.

First, we show in Fig 1 the instantaneous synchrotron spectra of the injected electrons. One can find that the MF decay case generally produces much weaker and harder synchrotron emission than that in the homogeneous MF case at the same time t . Thus the time-integrated spectrum should be harder. Then we calculate the time-integrated spectra up to different times (Fig 2) to illustrate how a harder spectrum in the low energy band is formed. From Fig 2, we can see that in the MF decay case the low energy index becomes softer with time and stabilizes at around ~ 1 at late time, harder than that in the homogeneous MF case.

In Fig 3, we show the time-integrated synchrotron spectrum, calculated over a duration from the electron injection up to 0.05 s, which is about $\sim 10^2 \tilde{t}_c$. Up to this time, the time-integrated spectrum does not vary any longer in the interesting energy range and becomes a "steady" state. One can see that the MF decay leads to harder low energy spectral slopes, compared with the homogeneous MF case. By changing the parameter values we can see how the resulted synchrotron spectrum varies.

From Fig 3 it can be seen that for the PLD case the low energy (below injection frequency) spectrum is mostly sensitive to the MF decay slope, α_B ; the spectrum is harder for larger α_B . For α_B approaching zero, the νF_ν spectral slope is close to the homogeneous MF case, $1/2$; if $\alpha_B \gtrsim 2$ the slope is close to the slow cooling slope, $4/3$. This is consistent with predicted in equation (13).

Fig 3 also shows that in the PLD the MF decay time scale and the Compton parameter do not sensitively affect the low energy slope. If the decaying time is larger, i.e., larger τ_B , the spectrum is close to the homogeneous MF case, but the spectral slope in the lowest energy range does not change much. Similarly, it can be seen that changing the Compton parameter Y_0 does not change much the spectral slope at the lowest energy end, while changing the normalization of the synchrotron spectrum.

In the ED case, the spectrum also becomes harder than the traditional homogeneous MF case, but similarly to the PLD case, the spectral slope tends towards $4/3$ and does not change much with varying MF decay time scale.

We also calculate the case of a spectrum softer than $1/2$, with $0 < \alpha_B < 2/3$ and without IC cooling (Fig. 4). These represent a small fraction of burst cases (Preece et al. 2000). From Fig 4, we can see that our numerical calculations indeed obtain a softer spectrum, roughly consistent with the prediction in equation (11).

Finally, we calculate the time-integrated IC spectrum, shown in Fig. 5. The IC spectral slope in the MF decay case in low energy band depends on the low energy part of the synchrotron spectrum, so it is also harder than the homogenous MF case. However, as in the case of a homogeneous MF, the IC component is usually dominated by the synchrotron component even in the high energy range, if the Compton parameter is not much larger than unity. This is mainly due to the KN suppression of the IC emission. The IC component in the MF decay case is even lower than that in the homogenous MF case, because of the fact that in the former case there are more soft seed photons that suffer less KN suppression.

The IC component only shows up if the Compton parameter is much larger than unity (see the case of $Y_0 = 5$), or the injected electron energy distribution is soft (so that the high energy synchrotron spectral tail is soft; see the case of $p = 2.8$). In Fermi-LAT observations, an IC component is not explicitly confirmed in most GRBs. But there are several GRBs showing an extra high energy component (Abdo et al. 2009a, 2009b), which might be the IC contribution.

5. DISCUSSION AND CONCLUSION

In this paper, we have assumed that the internal shock generated MF decays with distance from the shock front, and taking into account the electron cooling we calcu-

lated the synchrotron and IC emission. We find that the synchrotron spectrum at low energies (below the injection frequency) can be harder in this scenario than in the traditional scenario with a homogeneous postshock MF. The observed GRB spectra with typical low energy slopes $\alpha \sim -1$ are best reproduced in our power-law decay (PLD) models when (i) the MF decay time is comparable to electron cooling time ($\tau_B \sim 1$), (ii) the IC cooling is not much weaker than synchrotron cooling ($Y_0 \sim 0.5$), and (iii) the temporal power-law decay index is $\alpha_B \sim 1.5$; or in our exponential decay (ED) models with $\tau_B \sim 1$. The low energy spectral index is most sensitive to the MF decay index in the PLD case. We also find that the spectrum would be softer than $\nu F_\nu \sim 1/2$ if the MF decays slope $0 < \alpha_B < 2/3$ and the IC cooling is negligible. These cases correspond to the marginal fast cooling cases (or even slow cooling for $1/2 < \alpha_B < 2/3$) and thus are less interesting. However, in the observations, a handful of bursts indeed have spectra softer than $1/2$ (Preece et al. 2000). So these MF decay cases producing softer spectra might correspond to these observed bursts. Our results suggest that the low energy slopes in the MF decay cases are not fixed values of $\alpha = -3/2$ or $\alpha = -2/3$ (corresponding to fast or slow cooling, respectively) any more, but vary from $-2 < \alpha < -2/3$ ($\nu F_\nu \propto \nu^{0-4/3}$), which accommodates the observations for the vast majority of GRBs.

In the present MF decay cases, the synchrotron characteristic frequency moves more rapidly towards lower frequencies, compared with the homogeneous MF case. The energy which an electron emits at a certain synchrotron frequency is much less due to the decrease of the synchrotron cooling rate. The IC cooling becomes relatively stronger as the synchrotron emission weakens. Subsequently, this generates a harder spectrum than that in the homogeneous MF case. However, the spectrum is unlikely to be harder than $\nu F_\nu \propto \nu^{4/3}$. Thus, for the relatively small fraction of observed GRBs with νF_ν low energy spectral index $> 4/3$, different effects may be at play, e.g. strong synchrotron self absorption, or photospheric emission (e.g., Rees & Mészáros 2005; Pe'er et al. 2006; Beloborodov 2010).

The IC radiation will generate an extra component in the high energy band. However, it is dominant only in the cases when the initial Compton parameter is large, $Y_0 \gg 1$. Since the observations do not show a significant high energy component for most GRBs, a high Y_0 is not the general case. A very soft electron distribution is conducive to the emergence of the IC component. Several Fermi GRBs showing an high energy component do have a soft spectral slope $\beta \lesssim -2.5$ above E_p (Abdo et al. 2009a, 2009b), suggesting a soft electron energy distribution.

Pe'er & Zhang (2006) consider the MF decay effect on GRB prompt emission in the internal shock model, assuming a sharp MF decay. To avoid the fast cooling problem, the cooling frequency is required to be around the typical synchrotron frequency ($\nu_c \sim \nu_m$). Thus the spectrum in the low energy bands in their model would be $\nu F_\nu \sim \nu^{4/3}$. In the present paper, we find that the MF decay with different power laws can generate a wide range of spectra with $\nu F_\nu \propto \nu^{0-4/3}$, which accommodates the data of the vast majority of GRBs. We also find that the

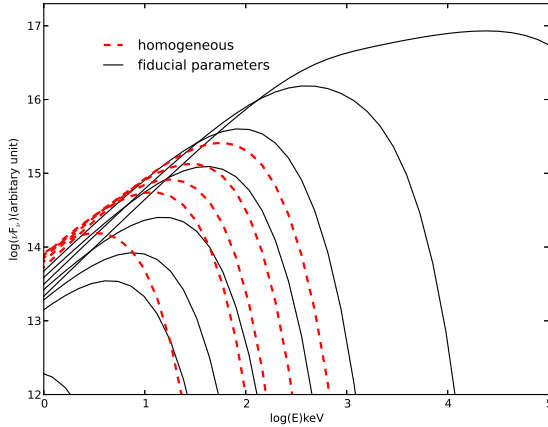


FIG. 1.— The instantaneous synchrotron spectra for the PLD and homogeneous MF cases. The fiducial parameters taken to be $\Gamma = 300$, $p = 2.3$, $Y_0 = 0.5$, $\alpha_B = 1.5$ and $\tau_B = 1.0$. The lines from right to left correspond to time $t = 1 \times 10^{-5}$ s, 1×10^{-4} s, 3×10^{-4} s, 4×10^{-4} s, 6×10^{-4} s, 8×10^{-4} s, 1×10^{-3} s, and 2×10^{-3} s, respectively. Note that the dashed and solid lines are superposed together for the times $< 4 \times 10^{-4}$ s.

IC cooling, although unimportant in the total energy loss of electrons, is important in shaping the spectrum in the low energy bands.

Uhm & Zhang (2013) recently have also considered the effect of an MF decay, and produce hard synchrotron spectra consistent with GRB observations. However, there are essential differences between their model and ours. Their MF decay time is comparable to the dynamical time of the outflow, $B \propto r^{-b}$ with $b \approx 1$, and their calculation keeps injecting electrons over a time which is longer by many orders of magnitude than the dynamical time at the point when the injection starts. Thus, the bulk electrons are injected at larger radii $r \sim 10^{16}$ cm (and hence small B and large cooling time) so they do not cool in the extremely fast cooling regime. In our work, by contrast, we have considered the internal shock model, and the MF decay time is smaller by many orders of magnitude than the dynamical time. The electron cooling time is required to be comparable to the MF decay time in order to avoid extreme fast cooling, and the synchrotron spectrum is further shaped by the suppression of synchrotron due to increasing IC cooling.

To reproduce the prompt GRB spectra in our model, the MF decay time should be comparable to the electron cooling time, $\tau_B \sim 1$, indicating a MF decay length much larger than the plasma skin depth, typically $ct_B \sim 10^5 c/\omega_p$ (see also Pe’er & Zhang 2006). This is different from the afterglow shock case (Gruzinov & Waxman 1999; Gruzinov 2001; Lemoine et al. 2013). For the prompt emission, if the GRB outflow is magnetized before the shock, this might lead to a relevant scale which is not the plasma scale but a much larger one.

We thank P. Veres, K. Kashiyama, D. Burrows, D. Fox, S. Gao, L. Uhm and B. Zhang for helpful discussions and the anonymous referee for helpful comments. We acknowledge partial support by the Chinese Natural Science Foundation (No. 11203067), Yunnan Natural Science Foundation (2011FB115) and

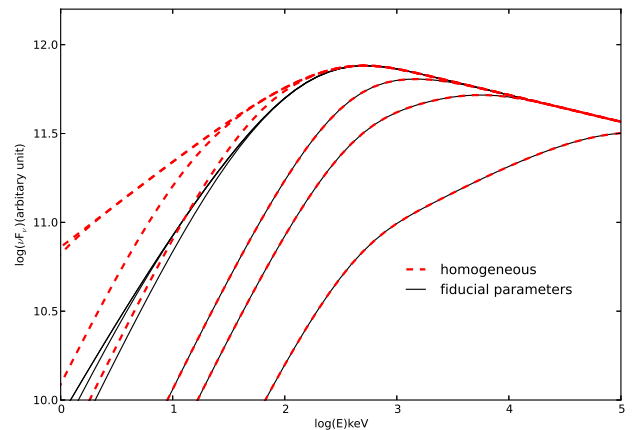


FIG. 2.— The time-integrated synchrotron spectra up to different times. The lines from right to left correspond to time $t = 1 \times 10^{-5}$ s, 5×10^{-5} s, 1×10^{-4} s, 5×10^{-4} s, 1×10^{-3} s, 5×10^{-3} s, and 1×10^{-2} s, respectively. Note that for $t > 5 \times 10^{-3}$ s, the spectra are unchanged with time and superposed together in both the PLD and homogeneous MF cases. And the dashed and solid lines are superposed together for $t < 5 \times 10^{-4}$ s.

the West Light Foundation of the CAS (XHZ); the NSFC (11273005), the MOE Ph.D. Programs Foundation, China (20120001110064), the CAS Open Research Program of Key Laboratory for the Structure and Evolution of Celestial Objects and the National Basic Research Program (973 Program) of China (Grant No. 2014CB845800)” (ZL); NASA NNX13AH50G (PM, XHZ); NSFC (No. 11133006) (JMB, XHZ); and NSFC (No. 11003014/A0303) (XWL)

REFERENCES

- Abdo, A. A., et al. 2009a, ApJ, 706, L138
 Abdo, A. A., et al. 2009b, Nature, 462, 331
 Band, D., et al. 1993, ApJ, 413, 281
 Beloborodov A. M., 2010, MNRAS, 407, 1033
 Chang, P., Spitkovsky, A., Arons, J., 2008, ApJ, 674, 378
 Cohen, E., Katz, J. I., Piran, T., Sari, R., Preece, R. D., & Band, D. L. 1997, ApJ, 488, 330
 Derishev, E. V., Kocharovsky, V. V., & Kocharovsky, V. V. 2001, A&A, 372, 1071
 Derishev, E. V. 2007, Ap&SS, 309, 157
 Ghisellini, G., Celotti, A., & Lazzati, D. 2000, MNRAS, 313, L1
 Gruzinov, A. 2001, ApJ, 563, L15
 Gruzinov, A., & Waxman, E. 1999, ApJ, 511, 852
 Keshet, U., Katz, B., Spitkovsky, A., & Waxman, E. 2009, ApJ, 693, L127
 Kumar, P., & Narayan, R. 2009, MNRAS, 395, 472
 Lemoine, M., 2013, MNRAS, 428, 845
 Lemoine, M., Li, Z. & Wang, X. Y., 2013, arXiv1305.3689
 Medvedev, M. V., Fiore, M., Fonseca, R. A., Silva, L. O., & Mori, W. B. 2005, ApJ, 618, L75
 Mészáros, P., Rees, M. J., & Papathanassiou, H. 1994, ApJ, 432, 181
 Mészáros, P. & Rees, M. J. 2000, ApJ, 530, 292
 Pe’er, A., & Zhang, B. 2006, ApJ, 653, 454
 Pe’er, A., Mészáros, P., & Rees, M. J. 2006, ApJ, 642, 995
 Pe’er, A., Zhang, B.-B., Ryde, F., et al. 2012, MNRAS, 420, 468

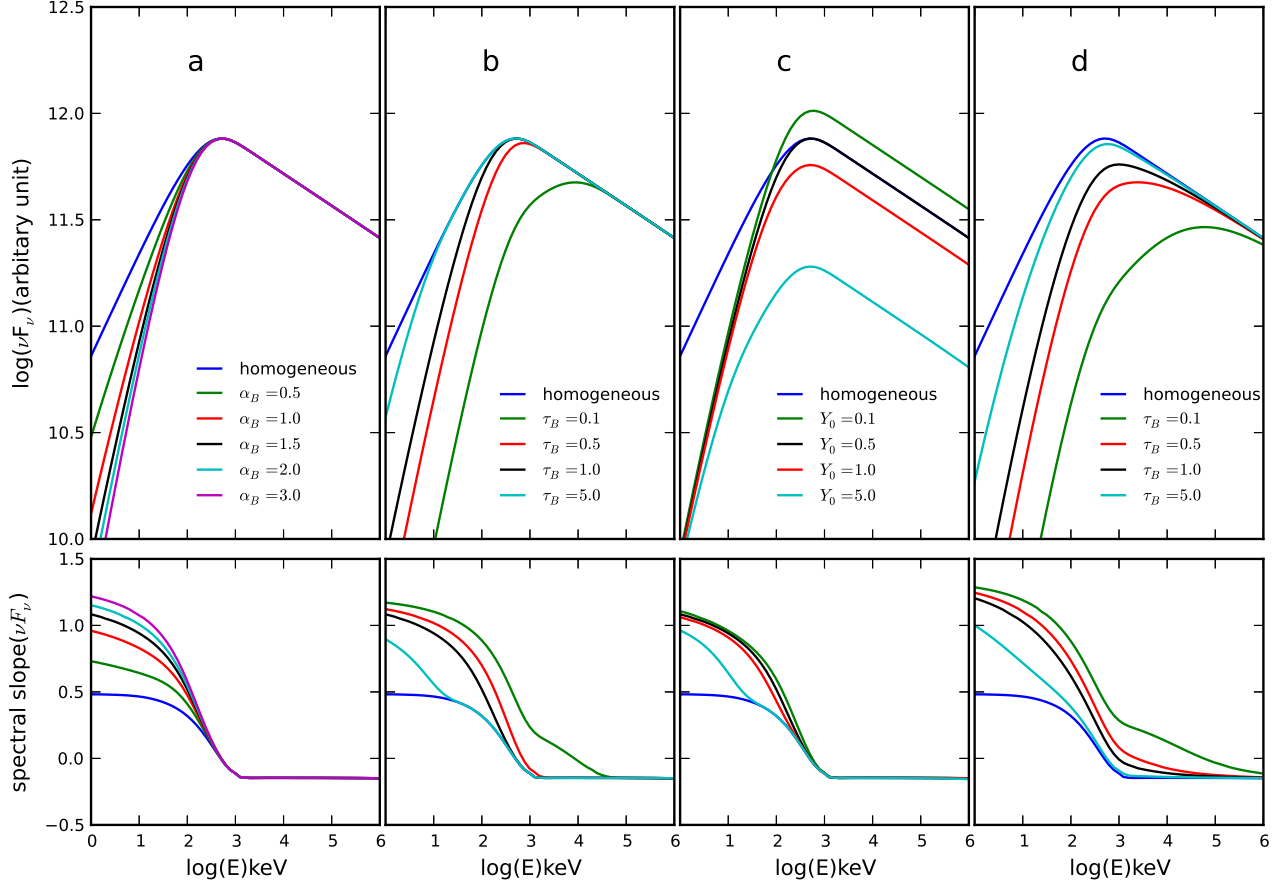


FIG. 3.— Time-integrated synchrotron spectrum. The label "homogeneous" indicates the homogeneous MF case. Panels a, b and c correspond to the PLD case, while panel d is the ED case. The bottom panels show the spectral slope as function of photon energy.

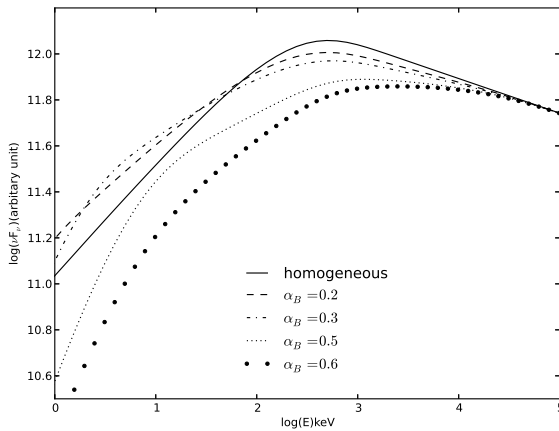


FIG. 4.— The PLD case with synchrotron spectra softer than $\nu F_\nu \propto \nu^{1/2}$. The α_B values are marked in the plot, and $\tau_B = 0.1$ and $Y_0 = 0$ are used. The other parameters not mentioned are taken to be the fiducial values.

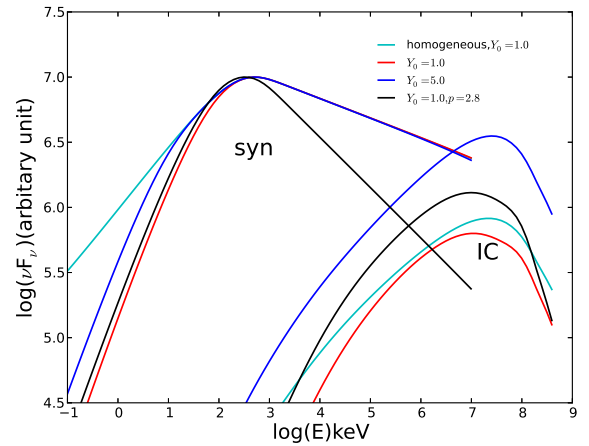


FIG. 5.— Time-integrated synchrotron and IC spectra for the PLD case. The parameters are marked on the plot, other parameters not mentioned having their fiducial values.

Piran, T., Sari, R., & Zou, Y.-C. 2009, MNRAS, 393, 1107
 Preece, R. D., Briggs, M. S., Mallozzi, R. S., Pendleton, G. N.,
 Paciesas, W. S., & Band, D. L. 2000, ApJS, 126, 19
 Rees, M. J., & Mészáros, P. 1994, ApJ, 430, L93

Rees, M. J., & Mészáros, P. 2005, ApJ, 628, 847
 Ryde, F., 2005, ApJL, 625, 95
 Ryde, F., et al., 2010, ApJL, 709, 172
 Silva, L. O., Fonseca, R. A., Tonge, J. W., Dawson, J. M., Mori,
 W. B., & Medvedev, M. V. 2003, ApJ, 596, L121

Tavani, M. 1996, ApJ, 466, 768

Uhm, L. & Zhang, B. 2013, arXiv:1303.2704